Journal of Organometallic Chemistry, 407 (1991) 391–412
Elsevier Sequoia S.A., Lausanne
JOM 21485

Cluster chemistry

LXVI*. Some iron–iridium clusters. X-ray structures of $Fe_2Ir(\mu_3\text{-}C_2Ph)(CO)_8(PPh_3)$, $FeIr_2(\mu_3\text{-}\eta^2\text{-}PhC_2C_2Ph)(CO)_7(PPh_3)_2$ and $Fe_2Ir(\mu_3\text{-}PhC_2PEt_3)(CO)_7(PEt_3)$

Michael I. Bruce, George A. Koutsantonis and Edward R.T. Tiekink

Jordan Laboratories, Department of Physical and Inorganic Chemistry, University of Adelaide, Adelaide, South Australia 5001 (Australia)

(Received October 8th, 1990)

Abstract

Reactions between $Ir(C_2Ph)(CO)_2(PPh_3)_2$ and iron carbonyls ($Fe(CO)_5$, $Fe_2(CO)_9$) have given Fe–Ir clusters $Fe_2Ir(\mu_3\text{-}C_2Ph)(CO)_{9-n}(PPh_3)_n$ ($n = 1$ (**8**), 2) and $FeIr_2(\mu_3\text{-}PhC_2C_2Ph)(CO)_7(PPh_3)_2$ (**9**). The Rh analogue of **8** was obtained similarly. Substitution of Ir–PPh_3 by PEt_3, and addition of PEt_3 to C_α of the acetylide ligand in **8** gave zwitterionic $Fe_2Ir(\mu_3\text{-}PhC_2PEt_3)(CO)_8(PEt_3)$ (**12**), which on heating was converted to $Fe_2Ir(\mu_3\text{-}C_2Ph)(CO)_7(PEt_3)_2$ by migration of PEt_3 from C to Ir. Related complexes containing cluster-bonded PR_3 were obtained with PMe_2Ph and $P(OMe)_3$. Complexes **8**, **9** and **12** were fully characterised by X-ray crystallography.

Introduction

One of the largest subsets of mixed-metal clusters is that containing iron or ruthenium and cobalt; many of these complexes containing bridging alkyne, vinylidene or acetylide ligands are known. In contrast, little work has been reported on analogous complexes containing the heavier congener, iridium. Mixed Fe–Ir complexes are limited to the binuclear complexes $FeIr(\mu\text{-}PPh_2)(CO)_5(PPh_3)_2$ (**1**), obtained from $Li[Fe(CO)_4(PPh_2)]$ and *trans*-$IrCl(CO)(PPh_3)_2$ [2], the cationic $[FeIr(\mu\text{-}CF_2)(\mu\text{-}CO)(CO)_2(PMe_2Ph)_2(\eta\text{-}C_5H_5)]^+$ (**2**), from $[Fe(CF_2)(CO)_2(\eta\text{-}C_5H_5)]^+$ and *trans*-$IrCl(CO)(PMe_2Ph)_2$ [3], and the trinuclear cluster $Fe_2Ir(\mu\text{-}CO)_2(CO)_7(\eta\text{-}C_5Me_5)$ (**3**) prepared from $Fe_3(CO)_{12}$ and $\{IrCl(\mu\text{-}Cl)_2(\eta\text{-}C_5Me_5)\}_2$ [4]. Complex **1**

---

* For Part LXV, see ref. 1.

0022-328X/91/$03.50

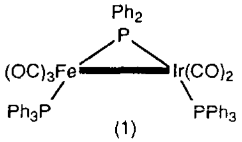

(1)

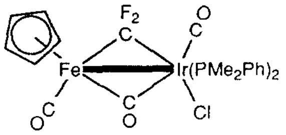

(2)

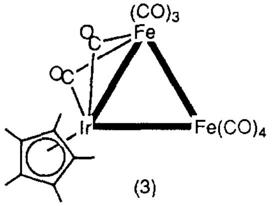

(3)

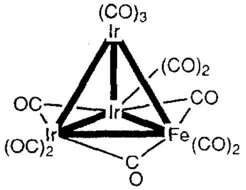

(5)

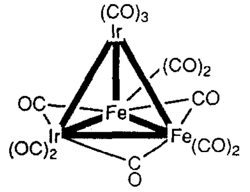

(4)

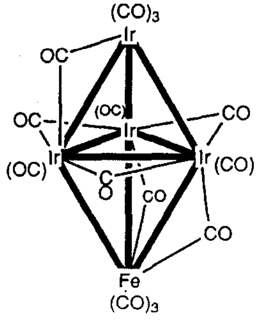

(6)

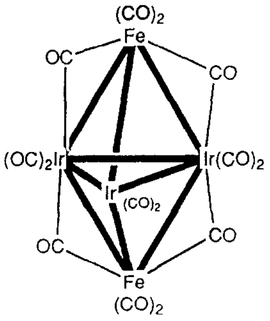

(7)

undergoes reversible CO addition/elimination reactions, and a series of hydrido complexes was obtained from its reaction with H_2. More recently, the anions $[Fe_2Ir_2(\mu\text{-}CO)_3(CO)_9]^{2-}$ (**4**), from $Fe_2(CO)_9$ and $[Ir(CO)_4]^-$, and $[FeIr_3(\mu\text{-}CO)_3(CO)_9]^-$ (**5**), formed by degradation of pentanuclear $[FeIr_4(\mu\text{-}CO)_6(CO)_9]^{2-}$ (**6**), which in turn was obtained with $[Fe_2Ir_3(\mu\text{-}CO)_4(CO)_{10}]^-$ (**7**) by reduction of $Fe(CO)_5$ and $Ir_4(CO)_{12}$ in ethanolic NaOH under CO, have been reported [5,6]. We have extended our studies of mono- and poly-nuclear complexes containing acetylide ligands to *trans*-$M(C_2R)(CO)(PPh_3)_2$ (M = Rh, Ir), and describe herein some of their chemistry with iron carbonyls. Some related chemistry of Fe–Rh complexes is also reported.

Results and discussion

Reactions of $Ir(C_2Ph)(CO)_2(PPh_3)_2$ with $Fe_2(CO)_9$

A mixture of $Ir(C_2Ph)(CO)_2(PPh_3)_2$ and $Fe_2(CO)_9$ reacts readily in refluxing tetrahydrofuran to give a mixture of four products (Scheme 1). Initial chromatographic separation afforded pure fractions containing $Fe(CO)_4(PPh_3)$ and the trinuclear cluster $Fe_2Ir(\mu_3\text{-}\eta^2\text{-}C_2Ph)(CO)_8(PPh_3)$ (**8**) in 33% yield. Fractional crystallisation of the band eluted last separated the di-iridium-iron cluster, $FeIr_2(\mu_3\text{-}\eta^2\text{-}PhC_2C_2Ph)(CO)_7(PPh_3)_2$ (**9**) (isolated in only low yield) from $Fe_2Ir(\mu_3\text{-}\eta^2\text{-}C_2Ph)(CO)_7(PPh_3)_2$ (**10**). These three complexes were formulated by a combination of microanalytical and spectroscopic techniques; the molecular structures of **8** and **9** were determined by X-ray crystallography.

Structure of $Fe_2Ir(\mu_3\text{-}\eta^2\text{-}C_2Ph)(CO)_8(PPh_3)$ (8)

The molecular structure of **8** is shown in Fig. 1 and important bond parameters are given in Table 1. The iridium and iron atoms adopt a triangular arrangement with the two iridium–iron distances being essentially equal (Ir–Fe(1) 2.701(1) and Ir–Fe(2) 2.693(1) Å). These values are similar to the value found for the non-CO bridged vector in $(\eta^5\text{-}C_5Me_5)IrFe_2(CO)_9$ (**3**) (Ir–Fe(2) 2.698(7) Å) [4] and significantly shorter than the Ir–Fe bond (2.960(1) Å) in $FeIr(\mu\text{-}PPh_2)(CO)_5(PPh_3)_2$ (**1**) [2]. The Fe–Fe separation in complex **8** (2.483(2) Å) is shorter than the analogous distance in **3** as expected from the presence of a bridging acetylide group in the

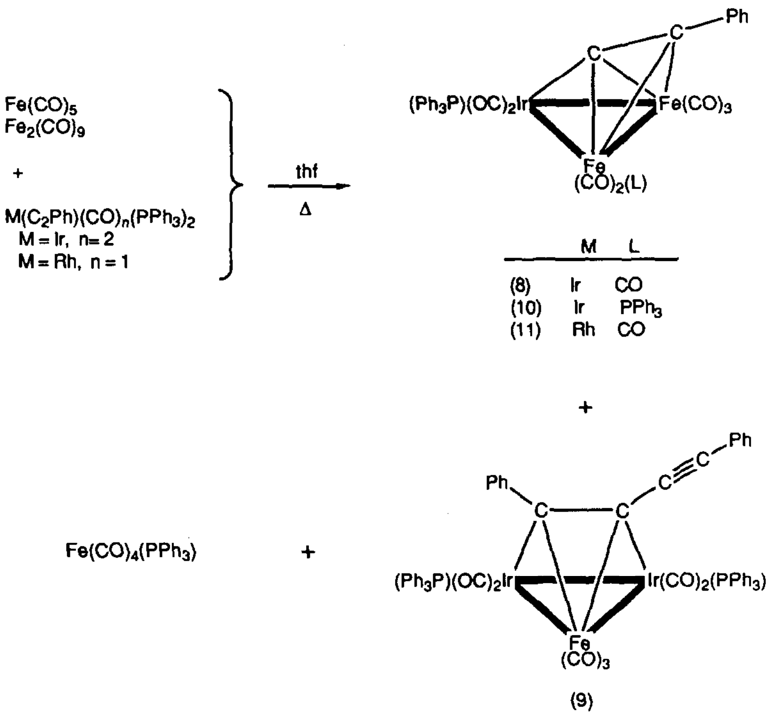

Scheme 1

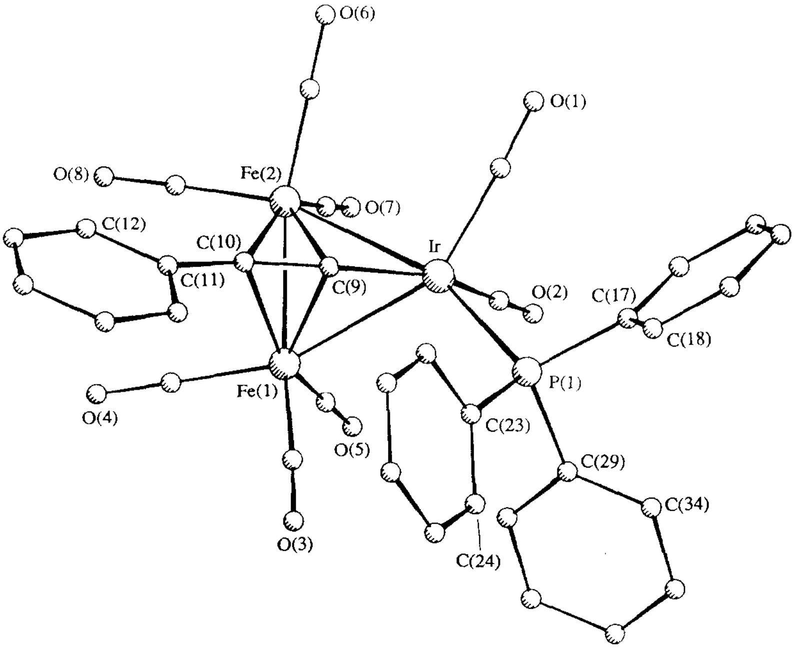

Fig. 1. Molecular structure and crystallographic numbering scheme for $Fe_2Ir(\mu_3\text{-}C_2Ph)(CO)_8(PPh_3)$ (**8**).

former complex. The Ir–P(1) distance (2.351(2) Å) is close to that observed in **1** (2.349(2) Å) for the terminal Ir–PPh_3 bond. The bridging acetylide ligand adopts the familiar μ_3-η^2- $\perp$ bonding mode with the C≡C and Ir–C_α distances (1.29(1) and 1.934(7) Å, respectively) consistent with those found in other homo- and heterometallic μ_3-η^2-acetylide clusters [7]. The bridging acetylide ligand is symmetrically arranged with respect to the two iron atoms (Fe(1)–C(9), C(10) 2.050(8), 2.133(8) Å; Fe(2)–C(9), C(10) 2.087(7), 2.098(7) Å). Coordination at the metal atoms is completed by two carbonyl ligands on Ir (Ir–CO 1.894 Å av.; Ir–C–O 176.8° av.) and three on each Fe (Fe–CO 1.771 Å av.; Fe–C–O 177.5° av.).

Table 1

Significant bond distances (Å) and angles (°) in complex **8**

Ir–Fe(1)	2.701(1)	Ir–Fe(2)	2.693(1)
Fe(1)–Fe(2)	2.483(2)	Ir–P(1)	2.351(2)
Ir–C(9)	1.934(7)	Fe(1)–C(9)	2.050(8)
Fe(2)–C(9)	2.087(7)	Fe(1)–C(10)	2.133(8)
Fe(2)–C(10)	2.098(7)	C(9)–C(10)	1.29(1)
Fe(1)–Ir–Fe(2)	54.8(1)	Fe(1)–Ir–P(1)	104.7(1)
Fe(2)–Ir–P(1)	153.6(1)	Ir–Fe(1)–Fe(2)	62.4(1)
Ir–Fe(2)–Fe(1)	62.7(1)	Ir–C(9)–C(10)	152.9(6)
Fe(1)–C(9)–Fe(2)	73.7(3)	Fe(1)–C(9)–C(10)	75.5(5)
Fe(2)–C(9)–C(10)	72.5(5)	Fe(1)–C(10)–Fe(2)	71.8(2)
Fe(1)–C(10)–C(9)	68.5(5)	Fe(2)–C(10)–C(9)	71.5(4)
C(9)–C(10)–C(11)	143.7(7)		

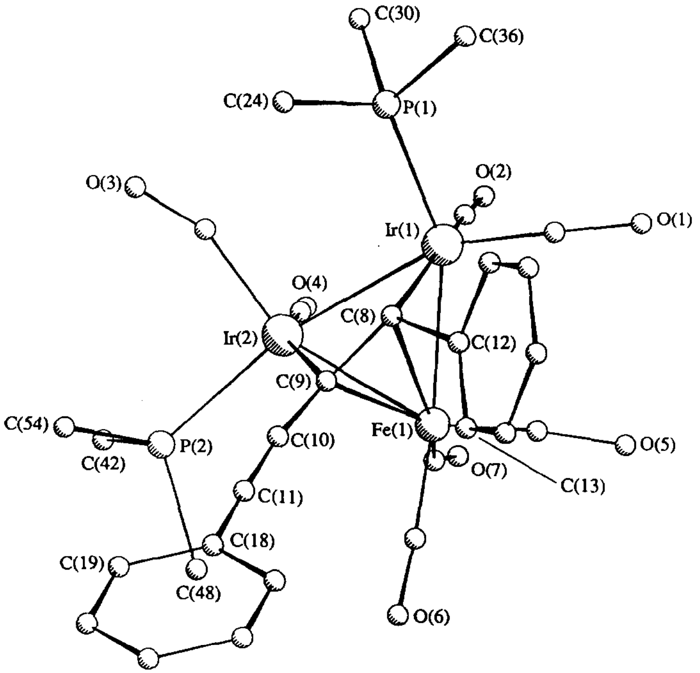

Fig. 2. Molecular structure and crystallographic numbering scheme for $FeIr_2(\mu_3\text{-}\eta^2\text{-}PhC_2C_2Ph)(CO)_7(PPh_3)_2$ (**9**). For reasons of clarity, only *ipso* carbons of the phosphorus-bonded phenyl groups are shown.

Complex **8** is electron-precise, and may be considered either as a substituted 48e triangular Fe_2Ir cluster, or as a trigonal bipyramidal C_2Fe_2Ir system with six skeletal electron pairs (SEP).

Spectroscopic data obtained for complex **8** are in accord with the crystallographically determined structure. Its solution IR spectrum showed only seven terminal $\nu(CO)$ bands. Resonances found at δ 174.5 and 212.1 in the $^{13}C\{^1H\}$ NMR spectrum were assigned to carbonyl ligands on the iridium and iron atoms, respectively, by comparison with similar resonances in the related complexes $FeRh(\mu\text{-}PPh_2)(CO)_4(PEt_3)_2$ [2] and $Ir_4(\mu\text{-}CO)_3(CO)_7(\eta^4\text{-}C_8H_{12})$ [8]. Observation of only two CO resonances suggests that the carbonyl groups on both metals are fluxional at ambient temperature or are accidentally equivalent; the former is more likely. However, CO ligands are not exchanged between Fe and Ir. The C_α (δ 165.5, s) and C_β (δ 99.6, s) signals were in environments similar to those found for other $\mu_3\text{-}\eta^2$-acetylide clusters [9]. A resonance at δ 14.9 in the $^{31}P\{^1H\}$ NMR spectrum was assigned to PPh_3 (cf δ 14.0 for Ir–PPh_3 in the related complex, $FeIr(\mu\text{-}PPh_2)(CO)_5(PPh_3)_2$ [2]). The FAB mass spectrum showed a molecular ion at *m/z* 892 which fragmented by loss of the eight CO ligands.

Structure of $FeIr_2(\mu_3\text{-}\eta^2\text{-}PhC_2C_2Ph)(CO)_7(PPh_3)_2$ *(9)*

The molecular structure of **9** is shown in Fig. 2; Table 2 collects significant bond parameters. Unfortunately, the accuracy of the determination only allowed the atom connectivities to be determined. The three metal atoms form a triangular arrange-

Table 2

Significant bond distances (Å) and angles (°) in complexes **9** and **12** [a]

	9	**12**	
Ir(1)-Ir(2)	2.743(4)	2.662(2)	Ir-Fe(1)
Ir(1)-Fe(1)	2.613(8)	2.642(2)	Ir-Fe(2)
Ir(2)-Fe(1)	2.627(8)	2.538(3)	Fe(1)-Fe(2)
Ir(1)-P(1)	2.33(2)	2.371(4)	Ir(1)-P(1)
Ir(2)-P(2)	2.36(2)	–	–
Ir(1)-C(8)	1.92(5)	2.06(2)	Ir-C(10)
Fe(1)-C(8)	2.18(5)	2.09(1)	Fe(2)-C(10)
Ir(2)-C(9)	2.18(5)	1.86(2)	Fe(1)-C(9)
Fe(1)-C(9)	2.17(5)	2.08(2)	Fe(2)-C(9)
C(8)-C(9)	1.40(2)	1.48(1)	C(9)-C(10)
C(8)-C(12)	1.66(6)	1.53(2)	C(10)-C(11)
C(9)-C(10)	1.44(7)	1.86(2)	C(9)-P(2)
C(10)-C(11)	1.22(7)	–	–
C(11)-C(18)	1.35(7)	–	–
Ir(2)-Ir(1)-Fe(1)	58.7(2)	57.2(1)	Fe(1)-Ir-Fe(2)
Ir(1)-Ir(2)-Fe(1)	58.2(2)	61.0(1)	Ir-Fe(1)-Fe(2)
Ir(1)-Fe(1)-Ir(2)	63.1(2)	61.8(1)	Ir-Fe(2)-Fe(1)
P(1)-Ir(1)-Ir(2)	100.6(4)	167.5(1)	P(1)-Ir-Fe(1)
P(1)-Ir(1)-Fe(1)	149.0(5)	110.4(1)	P(1)-Ir-Fe(2)
Ir(1)-C(8)-Fe(1)	79(2)	79.2(5)	Ir-C(10)-Fe(2)
Ir(1)-C(8)-C(9)	119(4)	102.3(7)	Ir-C(10)-C(9)
Fe(1)-C(8)-C(9)	71(3)	68.8(5)	Fe(2)-C(10)-C(9)
Ir(2)-C(9)-Fe(1)	74(2)	80.2(1)	Fe(1)-C(9)-Fe(2)
Ir(2)-C(9)-C(8)	100(4)	113.0(6)	Fe(1)-C(9)-C(10)
Fe(1)-C(9)-C(8)	72(3)	69.6(6)	Fe(2)-C(9)-C(10)
Ir(2)-C(9)-C(10)	127(3)	128.6(1)	Fe(1)-C(9)-P(2)
Fe(1)-C(9)-C(10)	126(3)	127.7(2)	Fe(2)-C(9)-P(2)
C(8)-C(9)-C(10)	132(5)	117.1(6)	C(10)-C(9)-P(2)
C(9)-C(10)-C(11)	174(5)	–	–
C(10)-C(11)-C(18)	172(6)	–	–

[a] Although the numbering systems for the two complexes necessarily differ, entries in the same rows compare like parameters.

ment in which the Ir-Fe distances (2.613(8) and 2.617(8) Å) are similar to those found in **8** and **3**. The homometallic bond distance (Ir(1)—Ir(1) 2.743(4) Å) is comparable to the average Ir-Ir bond length (2.73 Å av.) found in $Ir_4(\mu\text{-}CO)_3(CO)_7(\eta^4\text{-}C_8H_{12})$ [8]. The seven CO groups are disposed two to each Ir atom and three to the Fe atom. The two phosphorus atoms are essentially *trans* to each other along the Ir-Ir vector and with bond lengths (Ir(1)-P(1) 2.33(2) and Ir(2)-P(2) 2.36(2) Å) similar to those found in the previously mentioned complexes.

The most interesting feature of complex **9** is the presence of the μ_3-η^2-1,4-diphenylbuta-1,3-diyne ligand, which is attached to the $FeIr_2$ cluster by one of the two C≡C triple bonds (Ir(1)-C(8) 1.92(5), Ir(2)-C(9) 2.18(5), Fe-C(8) 2.18(5), Fe-C(9) 2.17(5) Å). The coordination is not symmetrical, but is best described as distorted μ_3-η^2-$\|$, presumably as a result of "freezing out" of the usual oscillatory motion of the alkyne ligand [10,11]. The coordinated C(8)-C(9) unit is longer (1.40(2) Å) than the C≡C bond (C(10)-C(11) 1.22(7) Å) found in the non-bonded half of the diyne; this part is essentially linear (C(9)-C(10)-C(11) 174(5)°), although the angle at C(9) is 132.4(5)°. This cluster is also an electron-precise 48e triangular system.

Limited spectroscopic data obtained for **9** include $^{31}P\{^1H\}$ resonances at δ 8.5 and -15.2 for the non-equivalent PPh_3 ligands; the FAB mass spectrum contained a molecular ion at m/z 1362; fragmentation included stepwise loss of six CO groups and a C_2Ph fragment.

The third complex was formulated as $Fe_2Ir(\mu_3\text{-}\eta^2\text{-}C_2Ph)(CO)_7(PPh_3)_2$ (**10**) from its spectroscopic properties. The solution IR spectrum contained a six-band terminal $\nu(CO)$ pattern. The ^1H NMR spectrum contained a multiplet at δ 7.1–7.7, assigned to the phenyl protons. Singlet resonances at δ 180.1 and 243.8 in the $^{13}C\{^1H\}$ NMR spectrum were assigned to CO ligands attached to Ir and Fe, respectively. While the C_α resonance was not observed, a signal at δ 80.0 was assigned to C_β. The $^{31}P\{^1H\}$ NMR was particularly informative and contained two resonances at δ -8.1 and 76.4. These were assigned to Ir–PPh_3 and Fe–PPh_3, respectively (cf δ 74.2 in $FeIr(\mu\text{-}PPh_2)(CO)_5(PPh_3)_2$ (**1**) [2]). The FAB mass spectrum contained a molecular ion at m/z 1126 which fragmented by loss of the CO groups. These data allowed the structure of **10** to be assigned as shown, one CO group on an Fe atom in **8** being replaced by PPh_3.

Reactions between $Ir(C_2Ph)(CO)_2(PPh_3)_2$ and $Fe(CO)_5$ afforded higher yields of **8** (25%) and **10** (15%) when carried out in refluxing tetrahydrofuran.

In the formation of **8**, one of the PPh_3 ligands originally attached to iridium is lost, it being scavenged by excess $Fe_2(CO)_9$ with formation of $Fe(CO)_4(PPh_3)$, isolated in 30% yield. An alternative reaction, with **8** to form **10**, also occurs to a small extent. It is unlikely that **10** is formed from $Ir(C_2Ph)(CO)_2(PPh_3)_2$ and $Fe(CO)_4(PPh_3)$, which is known to be relatively inert to substitution [12].

Of more interest is the acetylide coupling reaction which occurs in the formation of **9**. In addition to the well-known oxidative coupling of RC_2 by copper(II), the formation of complexes containing 1,4-diphenylbuta-1,3-diyne from phenylacetylide precursors has been reported in the thermolysis of $Mo(C_2Ph)(CO)_3(\eta\text{-}C_5H_5)$ at 110 °C to give structurally characterised $\{Mo(CO)_2(\eta\text{-}C_5H_5)\}_2(\mu\text{-}\eta^2\text{-}PhC_2C_2Ph)$ [13], and in the formation of $FeNi_2(\mu_3\text{-}\eta^2\text{-}PhC_2C_2Ph)(CO)_3(\eta\text{-}C_5H_5)_2$ in the reaction between $Fe_2(CO)_9$ and $Ni(C_2Ph)(PPh_3)(\eta\text{-}C_5H_5)$ [14]. It is not possible to say what stage coupling occurs relative to the formation of the mixed-metal cluster. However, formation of binuclear iridium complexes occurs on heating several mononuclear systems [15]; subsequent reaction with '$Fe(CO)_4$' has precedents in the reactions of $\{Ni(\eta\text{-}C_5H_5)\}_2(\mu\text{-}PhC_2C_2Ph)$ with $Fe_2(CO)_9$ [16].

Preparation of $Fe_2Rh(\mu_3\text{-}\eta^2\text{-}C_2Ph)(CO)_8(PPh_3)$ (11)

A suspension of $Rh(C_2Ph)(CO)(PPh_3)_2$ and $Fe_2(CO)_9$ in tetrahydrofuran rapidly darkened to red when heated at 60 °C for a short time. Preparative TLC enabled the isolation of two major products, namely $Fe_3(CO)_{12}$ and $Fe_2Rh(\mu_3\text{-}\eta^2\text{-}C_2Ph)(CO)_8(PPh_3)$ (**11**). The latter was formulated on the basis of microanalytical and spectroscopic data. The IR spectrum of **11** was similar to that of complex **8**. The ^1H NMR spectrum contained a multiplet at δ 7.32 assigned to the phenyl proton resonances. The phenyl carbon resonances of **11** were found between δ 128–134 in the $^{13}C\{^1H\}$ NMR spectrum. The only other signal found in this spectrum was a singlet at δ 212.1 assigned to the Fe-bonded CO groups. The $^{31}P\{^1H\}$ NMR spectrum contained a doublet at δ 15.6 ($J(RhP)$ 122 Hz); this value is comparable to that observed in $RhRu_3(\mu_3\text{-}PPh)(\mu_2\text{-}CO)(CO)_8(PPh_3)$ (δ(Rh–PPh_3) 30.9, $J(RhP)$ 128

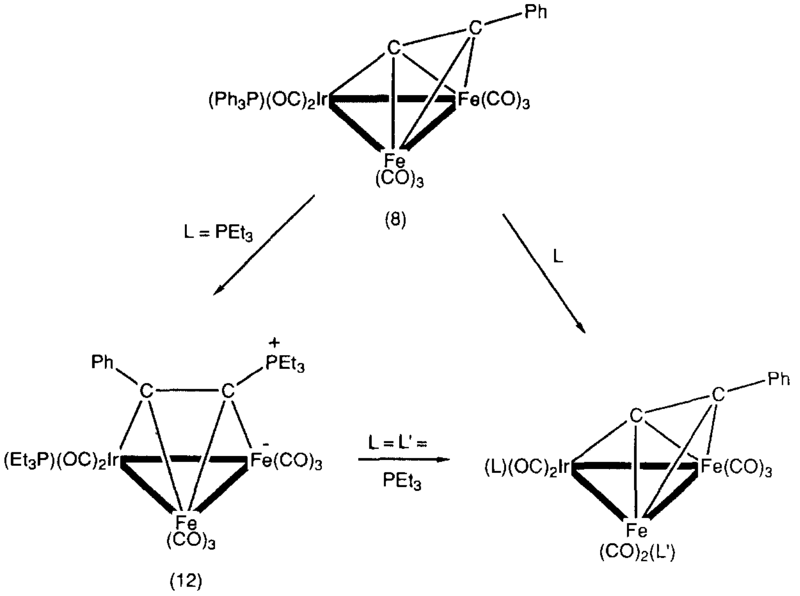

	L	L'
(13)	PPh_3	PEt_3
(14)	PEt_3	PEt_3
(15)	PEt_3	CO
(16)	PMe_2Ph	PMe_2Ph
(17)	PPh_3	$P(OMe)_3$
(18)	$P(OMe)_3$	$P(OMe)_3$

Scheme 2

Hz) [17]. A weak molecular ion was found at m/z 802 in the FAB mass spectrum; other ions formed by loss of up to eight CO groups were also present.

*Reactivity of $Fe_2Ir(\mu_3\text{-}C_2Ph)(CO)_8(PPh_3)$ (**8**)*

We have briefly explored the reactivity of **8** towards tertiary phosphines and phosphites (Scheme 2).

(a) With PEt_3. Treatment of a solution of **8** in THF at room temperature with a two-fold excess of PEt_3 gave three compounds: the zwitterionic complex $Fe_2Ir(\mu_3\text{-}\eta^2\text{-}PhC_2PEt_3)(CO)_8(PEt_3)$ (**12**) and the CO- and PPh_3-substitution products $Fe_2Ir(\mu_3\text{-}\eta^2\text{-}C_2Ph)(CO)_7(PEt_3)(PPh_3)$ (**13**) and $Fe_2Ir(\mu_3\text{-}\eta^2\text{-}C_2Ph)(CO)_7(PEt_3)_2$ (**14**). Complexes **12**, **13** and **14** were identified by the usual spectroscopic and microanalytical techniques and in the case of **12**, by X-ray structure analysis.

Structure of $Fe_2Ir(\mu_3\text{-}\eta^2\text{-}PhC_2PEt_3)(CO)_8(PEt_3)$ (12)

The molecular structure of **12** is shown in Fig. 3. Important bond parameters are given in Table 2, where they may be compared with related features in **9**. Attack of PEt_3 at C_α of the phenylacetylide unit in **8** has given an alkyne bonded to the Fe_2Ir cluster in the $\mu_3\text{-}\eta^2\text{-}\|$ mode, with C(9)–C(10) approximately parallel to the Fe(1)–Ir

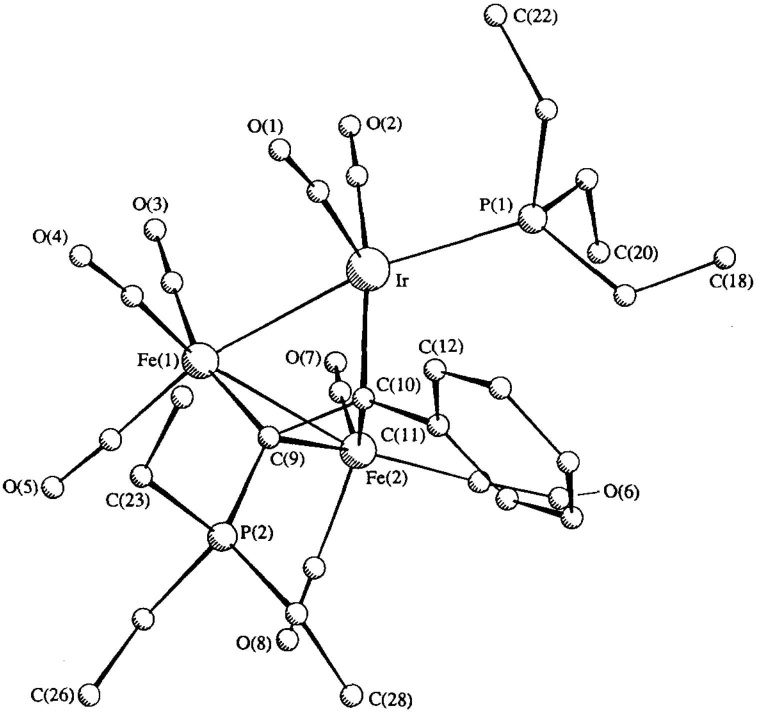

Fig. 3. Molecular structure and crystallographic numbering scheme for $Fe_2Ir(\mu_3\text{-}PhC_2PEt_3)(CO)_7(PEt_3)$ (**12**).

vector (Fe(1)–C(9) 1.86(2), Ir(1)–C(10) 2.06(2) Å). The Fe(2)–π-C_2 distances (both ca 2.08 Å) lie within the normal range of such distances [7]. The P(2)–C(9) distance of 1.86(2) Å may be compared to the value of 1.76(2) Å found in $Os_3(\mu\text{-}H)(\mu_3\text{-}\eta^2\text{-}HC_2PMe_2Ph)(CO)_9$ [18], and to the P–C(sp^2) distances of ca. 1.80 Å in related phosphonium salts [19]. The C(9)–C(10) separation (1.48(1) Å) is considerably longer than that found in **9**.

The spectroscopic data obtained for **12** are readily interpreted in terms of the solid-state structure. The IR spectrum contains four terminal ν(CO) absorptions. The ^{1}H NMR spectrum indicated substitution of the Ir–PPh_3 ligand by PEt_3, as well as addition of PEt_3 to the acetylide: multiplets centered on δ 0.91 and 1.13 were assigned to the CH_3 resonances of the PEt_3 moieties while the methylene groups gave multiplets centred on δ 1.43 and 1.70. The remaining multiplet at δ 7.15 was assigned to the phenyl protons of the alkyne ligand. Two resonances were observed in the $^{31}P\{^1H\}$ NMR spectrum at δ −10.2 and 38.3. The former signal is assigned to the Ir–PEt_3 resonance (cf. δ(Ir–PEt_3) −8.5 in (dppe)Rh(μ-H)$_3$Ir(PEt_3)$_3$ [20]) while the latter signal is assigned to the phosphonium centre on the basis of its low field position [21]. The FAB mass spectrum of **12** contained a molecular ion at *m/z* 866 which fragmented by stepwise loss of the eight CO groups. The strong metal-free ion at *m/z* 219 was assigned to $[PEt_3C_2Ph]^+$.

Formal electron book-keeping puts a positive charge on P(2) and negative charge on Fe(1). The reaction may be considered as addition of the 2e donor ligand to the *closo* C_2Fe_2Ir skeleton in **8** resulting in the formation of a *nido* cluster with distorted square pyramidal geometry.

The minor products from the reaction of **8** with PEt_3 were isolated by crystallisation after thin-layer chromatographic separation. Complexes **13** and **14** had very similar IR spectra containing four terminal $\nu(CO)$ bands. The ^1H NMR spectrum of **13** contained multiplets at δ 0.91 and 1.58, assigned to the methyl and methylene protons, respectively, of the coordinated phosphine ligands and a multiplet at δ 7.42 assigned to the phenyl protons of the acetylide group. The $^{31}P\{^1H\}$ NMR spectrum of **13** contained two resonances at δ 5.8 and 22.3, the lower field resonance being assigned to $Ir-PPh_3$ and the higher field resonance to $Ir-PEt_3$. A similar trend in $^{31}P\{^1H\}$ chemical shifts were observed in complexes $[FeRh(\mu\text{-}PPh_2)(CO)_4(PR_3)]^-$ (R = Ph, Et) where assignment was aided by the observation of $^{103}Rh-P$ coupling [2]. The ^1H NMR spectrum of complex **14** contained multiplets at δ 1.16 and 2.10 which were assigned to the PEt_3 ligands and the phenyl protons resonated in the usual region. A singlet at δ 7.6 was observed in the $^{31}P\{^1H\}$ NMR spectrum of **14** and was assigned to two equivalent $Ir-PEt_3$ ligands. Complexes **13** and **14** gave molecular ions in their FAB mass spectra at *m/z* 982 and 838, respectively, each fragmenting by successive loss of seven CO groups.

Thermolysis of **12** (refluxing CH_2Cl_2) resulted in formation of **14** in 80% yield; this process could be followed by ^{31}P NMR spectroscopy. A minor product was $Fe_2Ir(\mu_3\text{-}C_2Ph)(CO)_8(PEt_3)$ (**15**), best prepared by direct carbonylation (25 atm, 80 °C, 3 h) of **14**. Complex **15** was identified spectroscopically, having a similar IR $\nu(CO)$ spectrum to that of complex **8**, containing six terminal $\nu(CO)$ bands. A high field resonance at δ −12.5 in the $^{31}P\{^1H\}$ NMR spectrum of **17** was assigned to $Ir-PEt_3$. Characterisation was supported by observation of a molecular ion at *m/z* 748 in the FAB mass spectrum of **15** and ions formed by stepwise loss of eight CO groups.

A ^{31}P NMR study of the reaction between **8** and PEt_3 suggested that the first product is the adduct $Fe_2Ir(\mu_3\text{-}PhC_2PEt_3)(CO)_8(PPh_3)$ [δ −5 ($Ir-PPh_3$), 40 (C_2PEt_3)]; the growth of a resonance at δ −7 (free PPh_3) as the reaction proceeds is accompanied by a decrease in the intensity of the free PEt_3 resonance at δ −20, corresponding to substitution of the $Ir-PPh_3$ ligand by PEt_3 to give **12**. Conversion of **12** to **14** corresponds to migration of PEt_3 from one vertex (C) to another (Fe) with concomitant loss of CO and conversion of the *nido*-octahedral cluster to one with trigonal bipyramidal geometry.

(b) With PMe_2Ph. Treatment of a solution of **8** in THF with about two equivalents of PMe_2Ph resulted in an immediate darkening in colour. Suitable work-up gave $Fe_2Ir(\mu_3\text{-}\eta^2\text{-}C_2Ph)(CO)_7(PMe_2Ph)_2$ (**16**) in 65% yield, readily identified by the usual spectroscopic and microanalytical techniques. The solution IR spectrum of **16** was similar to those of complexes **13** and **14** containing only four terminal $\nu(CO)$ bands. The multiplets at δ 1.97 and 7.68 in the ^1H NMR spectrum of **16** were assigned to the methyl resonances of the PMe_2Ph ligands and the phenyl groups of PMe_2Ph and C_2Ph, respectively. The $^{31}P\{^1H\}$ NMR spectrum of **16** contained a singlet at δ 16.0 which was assigned to two equivalent $Ir-PMe_2Ph$ resonances. The FAB mass spectrum contained a molecular ion at *m/z* 878 which fragmented by the usual sequential loss of seven CO groups.

(c) With $P(OMe)_3$. The reaction of **8** with two equivalents of $P(OMe)_3$ in THF at 45 °C gave, after thin-layer chromatographic separation, two major products. These were identified by the usual methods as $Fe_2Ir(\mu_3\text{-}\eta^2\text{-}C_2Ph)(CO)_7(PPh_3)\{P(OMe)_3\}$ (**17**) and $Fe_2Ir(\mu_3\text{-}\eta^2\text{-}C_2Ph)(CO)_7\{P(OMe)_3\}_2$ (**18**). The solution IR

spectra of **17** and **18** were similar to the spectra of **14** and **16** and contained only terminal ν(CO) bands. The doublet signals at δ 3.47 (J(PH) 8 Hz) and 3.65 (J(PH) 13 Hz) in the ^{1}H NMR spectra of **17** and **18**, respectively, were assigned to the methyl groups of the $P(OMe)_3$ ligands. The $^{31}P\{^1H\}$ NMR spectrum of **18** contained a singlet at δ 112.2 which was assigned to two equivalent $Ir-P(OMe)_3$ ligands. Both complexes gave molecular ions in their FAB mass spectra at m/z 988 [**17**] or 850 [**18**], each fragmenting by stepwise loss of the seven CO groups.

In neither of the above reactions (b) and (c) was any evidence obtained for the formation of the zwitterionic phosphonium isomers.

^{31}P NMR studies on some iron–iridium clusters

The ^{31}P NMR data gathered in the course of this work proved invaluable in formulating the cluster complexes obtained. The presence of dissimilar metals allowed conclusive assignments to be made. A metal effect was observed in the $M-PPh_3$ resonances in which the general trend was the shift to lower field in the sequence Ir > Rh > Fe. The Rh resonances were easily assigned on the basis of observed ^{103}Rh coupling. Iridium–PEt_3 chemical shifts ranged in value from δ -12.5 to 7.46 while $Ir-PPh_3$ shifts were found in the range δ -8.0 to 30.6. These ranges show considerable overlap but the $Fe-PPh_3$ resonance of **10** was at significantly lower field (δ 76.4). Complexes **16** and **18** had signals at δ 16.0 and 112.2, respectively, which were assigned to $Ir-PMe_2Ph$ and $Ir-P(OMe)_3$, respectively, and reflected the different basicity of the coordinated phosphines.

Conclusions

The reactions between $Ir(C_2Ph)(CO)_2(PPh_3)_2$ and iron carbonyls have afforded new trinuclear iron–iridium clusters by template coordination of $Fe(CO)_n$ fragments to the acetylide and condensation. In one of these clusters, $FeIr_2(\mu_3\text{-}\eta^2\text{-}PhC_2C_2Ph)(CO)_7(PPh_3)_2$, an oxidative coupling of two phenylacetylide moieties to form a 1,3-diyne has occurred. The complex $Fe_2Ir(\mu_3\text{-}C_2Ph)(CO)_8(PPh_3)$ (**8**) undergoes nucleophilic attack at C_α by PEt_3 and is substitutionally labile at the Ir atom towards relatively basic phosphines.

Reactions of **8** with PEt_3 resulted in nucleophilic addition of the phosphine to the α-carbon of the acetylide ligand affording the zwitterionic complex $Fe_2Ir(\mu_3\text{-}\eta^2\text{-}PhC_2PEt_3)(CO)_8(PEt_3)$ (**12**). Addition at C_2 competes with CO and PPh_3 substitution at the Ir centre (as found at Co in the analogous Co_2Fe complex [22]); no intermetallic migration occurs on heating, although migration from C to Ir is observed. We note that compared with **9**, addition of PEt_3 to the phenylacetylide ligand results in its taking up the opposite configuration, i.e. with C(9) bearing the phenyl group being attached to iron rather than iridium.

The reactivity of **8** may be rationalised in terms of the ready addition of nucleophiles to the 46e *closo* cluster to give 48e *nido* species.

Experimental

General conditions. General experimental conditions have been described earlier [23].

Starting materials. Literature methods were used to prepare $Ir(C_2Ph)(CO)_2(PPh_3)_2$ [24] and $Rh(C_2Ph)(CO)(PPh_3)_2$ [25]. Iron carbonyls ($Fe(CO)_5$ and $Fe_2(CO)_9$) and phosphines (PEt_3 and PMe_2Ph) were purchased from Strem Chemicals and used as received; $P(OMe)_3$ (Strem) was distilled from 4 Å molecular sieve before use. Hydrogen (Commonwealth Industrial Gases) and carbon monoxide (Matheson Gas Products) were commercial products. Orthophosphoric acid (H_3PO_4, sp.gr. 1.75) was obtained from BDH Chemicals.

Syntheses

A. Reactions of $Ir(C_2Ph)(CO)_2(PPh_3)_2$

(a) With $Fe_2(CO)_9$. A mixture of $Ir(C_2Ph)(CO)_2(PPh_3)_2$ (2140 mg, 2.45 mmol) and $Fe_2(CO)_9$ (1068 mg, 2.94 mmol) was heated in refluxing THF (60 ml) for 50 min. After filtration, the red solution was evaporated to dryness and the residue chromatographed (alumina, 3 × 20 cm). Elution with CH_2Cl_2/light petroleum (1/10) gave a light yellow fraction which was evaporated to dryness *in vacuo* and the residue crystallised (acetone/light petroleum) to give light-yellow crystals of $Fe(CO)_4(PPh_3)$ (390 mg, 31%), m.p. 198–199 °C. IR (cyclohexane): $\nu(CO)$ 2055m, 1985m, 1950vs cm^{-1} (Lit. [26] m.p. 201–203 °C. IR (CCl_4): $\nu(CO)$ 2059m, 1984m, 1946vs cm^{-1}). Further elution with CH_2Cl_2/light petroleum (1/4), followed by removal of solvent *in vacuo* and crystallisation (CH_2Cl_2/MeOH) gave dark red crystals of $Fe_2Ir(\mu_3\text{-}\eta^2\text{-}C_2Ph)(CO)_8(PPh_3)$ (**8**) (721 mg, 33%), m.p. > 150 °C (dec.). [Found: C, 45.82; H, 2.26; M (mass spectrometry), 892; $C_{34}H_{20}Fe_2IrO_8P$ calc: C, 45.81; H, 2.26%; M, 892]. IR $\nu(CO)$ (cyclohexane): 2072m, 2035s, 2022s, 2008s, 1981m, 1969m, 1952w; $\nu(CO)$ (THF): 2066m, 2029vs, 2015s, 1999vs, 1967m, 1957m cm^{-1}. ^1H NMR: $\delta(CDCl_3)$ 7.44 (m, Ph). $^{13}C\{^1H\}$ NMR: $\delta[CDCl_3, Cr(acac)_3]$ 99.6 (s, C_β); 128.2–134.2 (m, Ph); 165.5 (s, C_α); 174.5 (s, 2 × CO, Ir–CO); 212.1 (s, 6 × CO, Fe–CO). $^{31}P\{^1H\}$ NMR: $\delta(CH_2Cl_2)$ 14.9 (s, PPh_3). FAB MS: 892, $[M]^+$, 24; 864, $[M-CO]^+$, 100; 780, $[M-4CO]^+$, 17, 752, $[M-5CO]$, 7; 724, $[M-6CO]^+$, 68; 696, $[M-7CO]^+$, 54; 667, $[M-8CO]$, 8. Elution with CH_2Cl_2/light petroleum (10/1) gave an orange fraction which was evaporated to dryness and the residue crystallised (CH_2Cl_2/MeOH) to give an orange powder of $FeIr_2(\mu_3\text{-}\eta^2\text{-}PhC_2C_2Ph)(CO)_7(PPh_3)_2$ (**9**) (341 mg, 20%), m.p. 190 °C (dec.). [Found: C, 50.93; H, 2.93; M (mass spectrometry), 1363; $C_{59}H_{40}FeIr_2O_7P \cdot 0.5CH_2Cl_2$ calc: C, 50.84; H, 2.94%; M, 1363]. IR (CH_2Cl_2): $\nu(CO)$ 2055s, 2024s, 2006s, 1996m, 1978w, 1956w cm^{-1}. ^1H NMR: $\delta(CDCl_3)$ 5.31 (s, 1H, CH_2Cl_2); 7.41 (m, 40H, Ph). $^{31}P\{^1H\}$ NMR: $\delta(CH_2Cl_2$, 205 K) 8.46 (s, Ir–PPh_3); −15.24 (s, Ir–PPh_3). FAB MS: $1362^{\star}$, $[M]^+$, 22; 1334, $[M-CO]^+$, 7; 1306, $[M-2CO]^+$, 3; $1261^{\star}$, $[M-C_2Ph]^+$, 4; 1278, $[M-3CO]^+$, 100; 1250, $[M-4CO]^+$, 22; 1222, $[M-5CO]^+$, 60; 1194, $[M-6CO]^+$, 14. Reduction in volume of the supernatant and cooling (ca 10 °C) resulted in the separation of red crystals of $Fe_2Ir(\mu_3\text{-}\eta^2\text{-}C_2Ph)(CO)_7(PPh_3)_2$ (**10**) (64 mg, 2%), m.p. > 173 °C (dec.). [Found: C, 55.01; H, 3.73; M (mass spectrometry), 1126; $C_{51}H_{35}Fe_2IrO_7P_2$ calc: C, 54.41; H, 3.13%; M, 1126]. IR (CH_2Cl_2): $\nu(CO)$ 2042s, 2014(sh), 1997vs, 1965m, 1941m, 1920(sh) cm^{-1}. ^1H NMR: $\delta(CDCl_3)$ 7.1–7.7 (m, Ph). $^{13}C\{^1H\}$ NMR: $\delta[CDCl_3, Cr(acac)_3]$ 80.0 (s, C_β); 127.3–137.4 (m, Ph); 180.1 (s, Ir–CO); 213.8 (s, 6 × CO, Fe–CO); C_α not observed. $^{31}P\{^1H\}$ NMR: $\delta(CH_2Cl_2)$ −8.1 (s, Ir–PPh_3); 76.4 (s, Fe–PPh_3). FAB MS: 1126, $[M]^+$, 2; 1098, $[M-CO]^+$, 3; 1042, $[M-3CO]^+$, 68; 1014, $[M-4CO]^+$, 5; 986, $[M-5CO]^+$, 89; 958, $[M-6CO]^+$, 100; 930, $[M-7CO]^+$, 34. Further

evaporation of the supernatant and separation of the residue by preparative TLC (acetone/light petroleum, 1/4) afforded a major dark red band (R_f 0.68), after triple development; crystallisation (CH_2Cl_2/MeOH) gave a further crop of **10** (17 mg, > 1%).

(b) With $Fe(CO)_5$ at ambient temperature. A solution of $Ir(C_2Ph)(CO)_2(PPh_3)_2$ (101 mg, 0.116 mmol) and $Fe(CO)_5$ (0.05 ml, 0.38 mmol) in THF (10 ml) was stirred at ambient temperature for 4 d, after which time the reaction was adjudged complete (TLC). The resulting dark orange solution was evaporated to dryness and the residue separated by preparative TLC (acetone/light petroleum, 1/4, doubly developed) to give four bands. Band 1 (R_f 0.66, yellow, trace), not identified. Band 2 (R_f 0.62, red-brown) was crystallised (CH_2Cl_2/MeOH) to give dark red crystals of **8** (12 mg, 12%). Band 3 (R_f 0.46, orange) was crystallised (CH_2Cl_2/light petroleum) to give orange crystals of **9** (9 mg, 12%). Band 4 (baseline, brown), intractable. Bands 2 and 3 were identified by comparison of their IR ν(CO), FAB mass and $^{31}P\{^1H\}$NMR spectra with those of the samples prepared above.

(c) With $Fe(CO)_5$ at elevated temperature. A solution of $Ir(C_2Ph)(CO)_2(PPh_3)_2$ (100 mg, 0.114 mmol) and $Fe(CO)_5$ (0.05 ml, 0.38 mmol) in THF (10 ml) was heated at 100 °C for 30 min. Analysis of the reaction mixture (TLC) indicated that all the $Fe(CO)_5$ had been consumed leaving unreacted $Ir(C_2Ph)(CO)_2(PPh_3)_2$. A further portion of $Fe(CO)_5$ (0.05 ml, 0.38 mmol) was added and the reaction continued for a further 1 h. Evaporation and preparative TLC (acetone/light petroleum, 1/3) gave seven bands. Band 1 (R_f 0.86, colourless) was not identified. Band 2 (R_f 0.74, brown), $Fe(CO)_5$ (identified by IR ν(CO) spectrum). Band 3 (R_f 0.62, red-brown) was crystallised (CH_2Cl_2/MeOH) to give dark red crystals of **8** (25 mg, 25%). Band 4 (R_f 0.52, dark red) was crystallised (CH_2Cl_2/MeOH) to give dark red crystals of **10** (19 mg, 15%). Both bands were identified by comparison of their IR ν(CO), FAB mass and $^{31}P\{^1H\}$ NMR spectra with those of authentic samples prepared above. Bands 5 and 6 (R_f's 0.49 and 0.46, respectively) were present in trace amounts and not identified.

B. Reaction of $Rh(C_2Ph)(CO)(PPh_3)_2$ with $Fe_2(CO)_9$

A suspension of $Rh(C_2Ph)(CO)(PPh_3)_2$ (380 mg, 0.502 mmol) and $Fe_2(CO)_9$ (734 mg, 2.02 mmol) in THF (15 ml) was heated at 60 °C for 15 min, after which time the reaction was adjudged complete (TLC). The dark red reaction mixture was cooled and filtered to remove unreacted $Fe_2(CO)_9$ (90 mg, 12%). The filtrate was evaporated to dryness and the residue separated by preparative TLC (acetone/light petroleum, 1/4) giving ten bands. Band 1 (R_f 0.85, green), $Fe_3(CO)_{12}$ (2 mg, 0.2%) [IR ν(CO)]. Band 2 (R_f 0.62, colourless), trace, not identified. Band 3 (R_f 0.53, dark red-brown) was crystallised (CH_2Cl_2/MeOH) to give dark red crystals of $Fe_2Rh(\mu_3\text{-}\eta^2\text{-}C_2Ph)(CO)_8(PPh_3)$ (**11**) (105 mg, 26%), m.p. 155–156 °C. [Found: C, 50.59; H, 2.59; M (mass spectrometry), 802; $C_{34}H_{20}Fe_2O_8PRh$ calc: C, 50.91; H, 2.51%; M, 802]. IR (cyclohexane): ν(CO) 2068m, 2037s, 2019vs, 2011(sh), 1983m, 1973(sh), 1968m cm^{-1}. ^1H NMR: $\delta(CDCl_3)$ 7.32 (m, Ph). $^{13}C\{^1H\}$ NMR: $\delta[CDCl_3, Cr(acac)_3]$ 128.1–133.7 (m, Ph); 212.1 (s, Fe–CO); the remaining carbons were not observed. $^{31}P\{^1H\}$ NMR: $\delta(CH_2Cl_2)$ 15.6 [d, J(RhP) 122 Hz]. FAB MS: 802, $[M]^+$, 2; 774, $[M-CO]^+$, 3; 690, $[M-4CO]^+$, 100; 662, $[M-5CO]^+$, 2; 634, $[M-6CO]^+$, 32; 606 $[M-7CO]^+$, 26; 579, $[M-8CO]^+$, 8. The remaining bands contained trace amounts of unidentified materials.

*C. Reactions of $Fe_2Ir(\mu_3\text{-}\eta^2\text{-}C_2Ph)(CO)_8(PPh_3)$ (**8**) with some tertiary phosphines and phosphites*

(a) With PEt_3: (i) In THF at ambient temperature. A solution of **8** (102 mg, 0.114 mmol) in THF (20 ml) was treated with PEt_3 (0.05 ml, 0.34 mmol) and stirred at ambient temperature for 2 h, after which time the reaction was adjudged complete (the disappearance of the IR ν(CO) bands of **8** at 2066, 2020 and 1999 cm^{-1} was monitored). Evaporation of the dark red solution to dryness and fractional crystallisation of the residue (CH_2Cl_2/MeOH) gave dark red crystals of $Fe_2Ir(\mu_3\text{-}\eta^2\text{-}PhC_2PEt_3)(CO)_8(PEt_3)$ (**12**) (40 mg, 41%), m.p. 195–197 °C. [Found: C, 38.68, H, 4.06; *M* (mass spectrometry), 866; $C_{28}H_{35}Fe_2IrO_8P_2$ calc: C, 38.86; H, 4.08%; *M*, 866]. IR (CH_2Cl_2): ν(CO) 2038s, 1985vs, 1952s, 1915s cm^{-1}. ^1H NMR: $\delta(CDCl_3)$ 0.91 (m, (H, $IrP\text{-}CH_2CH_3$); 1.13 (m, 9H, $C_2P\text{-}CH_2CH_3$); 1.43 (m, 6H, $IrP\text{-}CH_2CH_3$); 1.70 (m, 6H, $C_2P\text{-}CH_2CH_3$); 7.15 (m, 5H, Ph). $^{31}P\{^1H\}$ NMR: $\delta(CH_2Cl_2)$ −10.2 (s, $Ir\text{-}PEt_3$); 38.3 (s, $C_2\text{-}PEt_3$). FAB MS: 866, $[M]^+$, 6; 839, $[(M-CO)+H]^+$, 5; 810, $[M-2CO]^+$, 12; 782, $[M-3CO]^+$, 100; 754, $[M-4CO]^+$, 66; 726, $[M-5CO]^+$, 12; 698, $[M-6CO]^+$, 25; 770, $[M-7CO]^+$, 27; 742, $[M-8CO]^+$, 26; 219, $[PEt_3C_2Ph]^+$, 81. The supernatant was evaporated to dryness and the residue separated by preparative TLC (acetone/light petroleum, 1/3) to give nine bands. Band 1 (R_f 0.94, colourless) gave solid PPh_3, identified by TLC and mixed m.p. Band 2 (R_f 0.58, red-pink) was crystallised (CH_2Cl_2/MeOH) to give dark red crystals of **12** (7 mg, 7%), identified from its IR ν(CO) and FAB mass spectra. Band 3 (R_f 0.55, red-brown) was crystallised (CH_2Cl_2/MeOH) to give dark red crystals of $Fe_2Ir(\mu_3\text{-}\eta^2\text{-}C_2Ph)(CO)_7(PEt_3)(PPh_3)$ (**13**) (12 mg, 11%), m.p. 194–195 °C. [Found: C, 47.41; H, 3.64; *M* (mass spectrometry), 982; $C_{39}H_{35}Fe_2IrO_7P_2$ calc: C, 47.72; H, 3.59%; *M*, 982]. IR (CH_2Cl_2): ν(CO) 2030s, 1983vs(br), 1945(sh), 1932m cm^{-1}. ^1H NMR: $\delta(CDCl_3)$ 0.91 (m, 9H, PCH_2CH_3); 1.58 (m, 6H, PCH_2CH_3); 7.42 (m, 20H, Ph). $^{31}P\{^1H\}$ NMR: $\delta(CH_2Cl_2)$ 5.8 (s, $Ir\text{-}PEt_3$); 22.3 (s, $Ir\text{-}PPh_3$). FAB MS: 982, $[M]^+$, 6; 954, $[M-CO]^+$; 3, 898, $[M-3CO]^+$, 100; 870, $[M-4CO]^+$, 4; 842, $[M-5CO]^+$, 6; 814, $[M-6CO]^+$, 90; 786, $[M-7CO]^+$, 11; 758, $[M-8CO]^+$, 7. Band 4 (R_f 0.49, brown-red) was crystallised (CH_2Cl_2/MeOH) to give dark-red crystals of $Fe_2Ir(\mu_3\text{-}\eta^2\text{-}C_2Ph)(CO)_7(PEt_3)_2$ (**14**) (8 mg, 8%), m.p. > 150 °C (dec.). [Found: C, 38.67; H, 4.17; *M* (mass spectrometry), 838; $C_{27}H_{35}Fe_2IrO_7P_2$ calc: C, 38.72; H, 4.21%; *M*, 838]. IR (CH_2Cl_2): ν(CO) 2027s, 1978vs(br), 1939(sh), 1922m cm^{-1}. ^1H NMR: $\delta(CDCl_3)$ 1.16 (m, 18H, PCH_2CH_3); 2.10 (m, 12H, PCH_2CH_3); 7.50 (m, 5H, Ph). $^{31}P\{^1H\}$ NMR: $\delta(CH_2Cl_2)$ 7.6 (s, $Ir\text{-}PEt_3$). FAB MS: 838, $[M]^+$, 22; 810, $[M-CO]^+$, 45; 782, $[M-2CO]^+$, 40; 754, $[M-3CO]^+$, 30; 726, $[M-4CO]^+$, 100; 698, $[M-5CO]^+$, 31; 670, $[M-6CO]^+$, 35; 642, $[M-7CO]^+$, 81. The remaining bands contained trace amounts and were not identified.

(ii) In CH_2Cl_2 at ambient temperature. A solution of **8** (40 mg, 0.045 mmol) in CH_2Cl_2 (5 ml) was treated with PEt_3 (0.9 ml of ca 0.1 mol l^{-1} solution in CH_2Cl_2, 0.09 mmol) and the resulting dark red solution was stirred for 59 h. Evaporation and preparative TLC (acetone/light petroleum, 1/4) afforded eight bands. Bands 1 and 2 (R_f's 0.42 and 0.36) gave **13** (6 mg, 14%) and **14** (11 mg, 29%), respectively.

(iii) In CH_2Cl_2 at 0 °C. A solution of **8** (30 mg, 0.034 mmol) in CH_2Cl_2 (5 ml) at 0 °C was treated with PEt_3 (0.75 ml of ca 0.1 mol l^{-1} solution in CH_2Cl_2, 0.075 mmol) and stirred for 9 h to give a dark red solution from which **13** (R_f 0.60; 15

mg, 45%) and **14** (R_f 0.54; 3 mg, 11%) were obtained (preparative TLC; acetone/light petroleum 1/4).

(iv) In CH_2Cl_2 at 0 °C under CO. A solution of **8** (26 mg, 0.029 mmol) in CH_2Cl_2 (20 ml) saturated with CO was treated with PEt_3 (0.65 ml of ca 0.1 mol l^{-1} solution in CH_2Cl_2, 0.065 mmol) and stirred under a CO atmosphere for 1 h. The solution was warmed to ambient temperature and stirred for 48 h. Evaporation and preparative TLC (acetone/light petroleum, 1/3) gave two bands (R_f 0.55 and 0.41), containing **12** (18 mg, 69%) and **13** (6 mg, 21%), respectively. Bands 1 and 2 were identified by comparison of their IR ν(CO) and FAB mass spectra with those of authentic samples.

(v) In CH_2Cl_2 with one equivalent of PEt_3. A solution of **8** (60 mg, 0.067 mmol) in CH_2Cl_2 (10 ml) was treated with PEt_3 (0.01 ml, 0.068 mmol) and stirred for 2 h. Evaporation and preparative TLC (acetone/light petroleum, 1/4) gave three bands. Band 1 (R_f 0.67, red) was crystallised (CH_2Cl_2/MeOH) to give dark-red crystals of **8** (35 mg, 58%). Band 2 (R_f 0.53, red) was further separated by preparative TLC (CH_2Cl_2/acetone/cyclohexane, 40/15/65) to give three bands. Band 2a (R_f 0.79, brown-red) gave solid **13** (11 mg, 17%). Band 2b (R_f 0.72, red) gave solid **12** (12 mg, 20%). Band 2c (R_f 0.66, red) gave solid **14** (2 mg, 4%). Bands 2a, 2b and 2c were identified by comparison of their $^{31}P\{^1H\}$ NMR and IR ν(CO) spectra with those of authentic samples.

(b) With PMe_2Ph: A solution of **8** (50 mg, 0.056 mmol) in THF (20 ml) was treated with PMe_2Ph (0.12 ml of ca 1 mol l^{-1} solution in THF, 0.12 mmol). An immediate darkening in colour to deep red was observed. After 40 min the solution was evaporated to dryness and the residue chromatographed (Florisil, 1 × 10 cm). Elution with light petroleum removed PMe_2Ph. Further elution with acetone/light petroleum (1/4), removal of the solvent *in vacuo* and crystallisation (CH_2Cl_2/heptane) afforded dark red crystals of $Fe_2Ir(\mu_3\text{-}\eta^2\text{-}C_2Ph)(CO)_7(PMe_2Ph)_2$ (**16**) (32 mg, 65%) m.p. 185–186 °C. [Found: C, 42.16; H, 3.12; *M* (mass spectrometry), 878. $C_{31}H_{27}Fe_2IrO_7P_2$ calc: C, 42.43; H, 3.10%; *M*, 878]. IR (CH_2Cl_2): ν(CO) 2032m, 1985s(br), 1948(sh), 1930w cm^{-1}. ^1H NMR: $\delta(CDCl_3)$ 1.97 (m, 12H, PCH_3); 7.68 (m, 15H, Ph). $^{31}P\{^1H\}$ NMR: $\delta(CH_2Cl_2)$ 16.0 (Ir–PMe_2Ph). FAB MS: 878, $[M]^+$, 8; 850, $[M-CO]^+$, 8; 794, $[M-3CO]^+$, 100; 738, $[M-5CO]^+$, 74; 710, $[M-6CO]^+$, 53; 682, $[M-7CO]^+$, 21.

(c) With $P(OMe)_3$: A solution of **8** (50 mg, 0.056 mmol) in THF (20 ml) was treated with $P(OMe)_3$ (0.80 ml of 0.113 mol l^{-1} solution in THF, 0.09 mmol) and stirred at ambient temperature for 2 h. The solution was heated at 45 °C and stirred for a further 17 h, during which time the colour changed from red-brown to orange. Evaporation and preparative TLC (acetone/light petroleum, 1/4) gave five bands of which two major bands were isolated. Band 1 (R_f 0.5, red) gave red crystals (Et_2O/light petroleum) of $Fe_2Ir(\mu_3\text{-}\eta^2\text{-}C_2Ph)(CO)_7(PPh_3)\{P(OMe)_3\}$ (**17**) (6 mg, 11%), m.p. 197–199 °C. [Found: C, 43.12; H, 3.05; *M* (mass spectrometry), 998; $C_{36}H_{29}Fe_2IrO_{10}P_2$ calc: C, 43.79; H, 2.96%; *M*, 988]. IR (cyclohexane): ν(CO) 2044s, 1999vs, 1965w, 1950m cm^{-1}. ^1H NMR: $\delta(CDCl_3)$ 3.47 [d, *J*(PH) 8 Hz, 9H, $POCH_3$]; 7.41 (m, 20H, Ph). FAB MS: 988, $[M]^+$, 3; 960, $[M-CO]^+$, 4; 904, $[M-3CO]^+$, 94; 845, $[M-5CO]^+$, 26; 820, $[M-6CO]^+$, 100; 792, $[M-7CO]^+$, 10. Band 2 (R_f 0.45, orange) gave orange crystals (Et_2O/light petroleum) of $Fe_2Ir(\mu_3\text{-}\eta^2\text{-}C_2Ph)(CO)_7\{P(OMe)_3\}_2$ (**18**) (34 mg, 72%), m.p. 203–205 °C. [Found: C, 29.58; H, 2.76; *M* (mass spectrometry), 850; $C_{21}H_{23}Fe_2IrO_{13}P_2$ calc: C, 29.70; H,

2.73%, M, 850]. IR (cyclohexane): ν(CO) 2048m, 2006(sh), 1998s, 1964w, 1949 cm^{-1}. ^{1}H NMR: δ($CDCl_3$) 3.65 [d, J(PH) 13 Hz, 18H, $POCH_3$]; 7.55 (m, 5H, Ph). ^{31}P{^{1}H} NMR: δ(CH_2Cl_2) 112.2 [s, Ir–P(OMe)$_3$]. FAB MS: 850, $[M]^+$, 6; 822, $[M-CO]^+$, 18; 794, $[M-2CO]^+$, 19; 766, $[M-3CO]^+$, 6; 748 $[M-4CO]^+$, 54; 720, $[M-5CO]^+$, 100; 692, $[M-6CO]^+$, 63; 651, $[M-7CO]^+$, 18.

*D. Pyrolysis of $Fe_2Ir(\mu_3\text{-}\eta^2\text{-}PhC_2PEt_3)(CO)_8(PEt_3)$ (**12**)*

A solution of **12** (20 mg, 0.013 mmol) in CH_2Cl_2 (20 ml) was heated at reflux point for 8 h while being purged with nitrogen. Evaporation and preparative TLC afforded four bands. Band 1 (R_f 0.88, orange) gave solid $Fe_2Ir(\mu_3\text{-}\eta^2\text{-}C_2Ph)(CO)_8(PEt_3)$ (**15**) (2 mg, 12%), identified from its IR ν(CO) and FAB mass spectra (below). Band 2 (R_f, 0.78, red) was not identified. IR (CH_2Cl_2): ν(CO) 2029s, 1983vs(br), 1942(sh), 1931w cm^{-1}. Band 3 (R_f 0.71, red) gave dark red crystals (CH_2Cl_2/MeOH) of **14** (15 mg, 80%), identified from its IR ν(CO) and FAB mass spectra.

*E. Carbonylation of $Fe_2Ir(\mu_3\text{-}\eta^2\text{-}C_2Ph)(CO)_7(PEt_3)_2$ (**14**)*

A solution of **14** (20 mg, 0.023 mmol) in cyclohexane (20 ml) was carbonylated in an autoclave (25 atm, 80 °C, 3 h) and the resulting brown-orange solution was filtered, evaporated to dryness and the residue separated by preparative TLC

Table 3

Crystal data and refinement details for complexes **8**, **9** and **12**

	8	**9**	**12**
Formula	$C_{34}H_{20}Fe_2IrO_8P$	$C_{59}H_{40}FeIr_2O_7P_2$	$C_{28}H_{35}Fe_2IrO_8P_2$
Mol. wt.	891.4	1363.1	865.4
Crystal system	monoclinic	monoclinic	triclinic
Space group	$P2_1/n$	$P2_1/c$	$P\bar{1}$
a, Å	12.441(3)	13.592(8)	10.518(5)
b, Å	14.538(2)	20.858(13)	10.648(5)
c, Å	18.236(5)	19.609(14)	14.547(5)
α, °	90	90	98.23(3)
β, °	96.40(2)	100.72(5)	93.00(3)
γ, °	90	90	97.85(4)
V, Å^3	3277.7	5462.2	1593.0
Z	4	4	2
D_c, g cm^{-3}	1.806	1.658	1.804
F(000)	1728	2640	852
μ, cm^{-1}	49.74	51.81	51.60
Transmission factors (max./min.)	0.259; 0.101	0.452; 0.229	0.530; 0.223
θ limits, °	1.0–22.5	1.0–20.0	1.0–22.5
No. of data collected	6158	6199	4473
No. of unique data	4290	5078	4171
No. of unique reflections used with $I \geqslant 2.5\sigma(I)$	3826	1687	2678
R	0.056	0.089	0.056
k	1.0	0.233	1.0
g	0.007	0.079	0.007
R_w	0.063	0.092	0.055

(acetone/light petroleum, 1/4) to give six bands. Only the major band (R_f 0.58, orange) was isolated and gave solid $Fe_2Ir(\mu_3\text{-}\eta^2\text{-}C_2Ph)(CO)_8(PEt_3)$ (**15**) (8 mg, 47%), m.p. > 150 °C (dec.). IR (CH_2Cl_2): ν(CO) 2064s, 2024vs, 1994s, 1963m, 1950m,

Table 4

Fractional atomic coordinates ($\times 10^5$ for Fe, Ir; $\times 10^4$ for remaining atoms) for $Fe_2Ir(\mu_3\text{-}C_2Ph)(CO)_8(PPh_3)$ (**8**)

Atom	*x*	*y*	*z*
Ir	17478(2)	15643(2)	-3648(2)
Fe(1)	27198(9)	19751(7)	-15761(6)
Fe(2)	19586(9)	4048(7)	-14916(6)
P(1)	2385(2)	2683(1)	509(1)
C(1)	1281(7)	665(6)	284(5)
O(1)	979(5)	90(5)	627(4)
C(2)	361(7)	2098(6)	-567(5)
O(2)	-488(5)	2394(5)	-719(4)
C(3)	3663(7)	2875(6)	-1295(5)
O(3)	4295(7)	3430(5)	-1139(5)
C(4)	3155(8)	1841(6)	-2470(5)
O(4)	3466(8)	1757(6)	-3026(4)
C(5)	1547(7)	2584(6)	-1883(5)
O(5)	747(6)	2980(5)	-2120(4)
C(6)	1743(6)	-652(6)	-1048(6)
O(6)	1585(6)	-1353(5)	-752(6)
C(7)	600(7)	694(6)	-1801(5)
O(7)	-286(5)	854(5)	-2038(4)
C(8)	2185(8)	-44(6)	-2358(6)
O(8)	2307(7)	-322(6)	-2931(4)
C(9)	3044(6)	1075(5)	-714(4)
C(10)	3590(6)	760(5)	-1223(5)
C(11)	4682(4)	502(4)	-1387(3)
C(12)	4836(4)	-91(4)	-1968(3)
C(13)	5878(4)	-272(4)	-2143(3)
C(14)	6767(4)	139(4)	-1738(3)
C(15)	6614(4)	732(4)	-1157(3)
C(16)	5572(4)	913(4)	-981(3)
C(17)	2052(3)	2430(4)	1433(3)
C(18)	2834(3)	2516(4)	2039(3)
C(19)	2578(3)	2304(4)	2745(3)
C(20)	1538(3)	2005(4)	2845(3)
C(21)	755(3)	1919(4)	2239(3)
C(22)	1012(3)	2132(4)	1533(3)
C(23)	3841(5)	2831(3)	613(5)
C(24)	4320(5)	3700(3)	638(5)
C(25)	5444(5)	3782(3)	748(5)
C(26)	6088(5)	2996(3)	832(5)
C(27)	5609(5)	2127(3)	807(5)
C(28)	4485(5)	2045(3)	697(5)
C(29)	1863(5)	3847(4)	336(3)
C(30)	1794(5)	4173(4)	-388(3)
C(31)	1503(5)	5086(4)	-541(3)
C(32)	1281(5)	5672(4)	29(3)
C(33)	1350(5)	5346(4)	752(3)
C(34)	1641(5)	4433(4)	905(3)

Table 5

Fractional atomic coordinates ($\times 10^4$) for $FeIr_2(\mu_3\text{-}PhC_2C_2Ph)(CO)_7(PPh_3)_2$ (**9**)

Atom	*x*	*y*	*z*
Ir(1)	6368(2)	1595(1)	3831(1)
Ir(2)	7171(3)	2724(1)	3471(1)
Fe	6695(9)	2557(4)	4698(4)
P(1)	6972(15)	882(8)	3090(9)
P(2)	7984(15)	3723(8)	3485(8)
C(1)	5979(47)	966(21)	4429(26)
O(1)	5583(38)	625(24)	4784(24)
C(2)	5062(23)	1705(36)	3293(30)
O(2)	4379(46)	1851(29)	3016(30)
C(3)	7600(53)	2415(31)	2663(21)
O(3)	8067(37)	2371(22)	2202(22)
C(4)	5896(23)	2952(33)	2953(29)
O(4)	5230(43)	3187(26)	2645(27)
C(5)	6238(50)	2104(27)	5335(26)
O(5)	5813(45)	1894(27)	5762(28)
C(6)	7236(52)	3137(26)	5313(27)
O(6)	7770(38)	3426(24)	5757(24)
C(7)	5685(34)	3084(23)	4381(28)
O(7)	4859(25)	3324(16)	4164(16)
C(8)	7603(40)	1757(20)	4458(26)
C(9)	8111(41)	2331(20)	4396(25)
C(10)	9075(47)	2565(27)	4729(26)
C(11)	9851(45)	2774(26)	5065(26)
C(12)	8163(37)	1368(16)	5162(25)
C(13)	8635(37)	1632(16)	5791(25)
C(14)	9158(37)	1238(16)	6309(25)
C(15)	9209(37)	579(16)	6198(25)
C(16)	8737(37)	315(16)	5568(25)
C(17)	8214(37)	709(16)	5050(25)
C(18)	10735(73)	2920(38)	5475(31)
C(19)	11417(73)	3320(38)	5232(31)
C(20)	12321(73)	3477(38)	5663(31)
C(21)	12543(73)	3234(38)	6338(31)
C(22)	11860(73)	2825(38)	6580(31)
C(23)	10956(73)	2678(38)	6149(31)
C(24)	8244(29)	873(19)	2917(16)
C(25)	8460(29)	917(19)	2252(16)
C(26)	9432(29)	1025(19)	2143(16)
C(27)	10188(29)	1189(19)	2700(16)
C(28)	9972(29)	1244(19)	3365(16)
C(29)	9000(29)	1136(19)	3474(16)
C(30)	6240(36)	832(18)	2219(24)
C(31)	5873(36)	1390(18)	1868(24)
C(32)	5300(36)	1351(18)	1200(24)
C(33)	5094(36)	754(18)	884(24)
C(34)	5461(36)	197(18)	1235(24)
C(35)	6034(36)	236(18)	1902(24)
C(36)	6990(31)	33(27)	3348(25)
C(37)	6105(31)	−278(27)	3418(25)
C(38)	6129(31)	−914(27)	3638(25)
C(39)	7040(31)	−1241(27)	3790(25)
C(40)	7925(31)	−931(27)	3721(25)
C(41)	7901(31)	−294(27)	3500(25)

Table 5 (*continued*)

Atom	x	y	z
C(42)	7387(35)	4265(16)	2789(22)
C(43)	7073(35)	4018(16)	2123(22)
C(44)	6702(35)	4428(16)	1574(22)
C(45)	6645(35)	5086(16)	1690(22)
C(46)	6959(35)	5333(16)	2356(22)
C(47)	7331(35)	4922(16)	2906(22)
C(48)	8032(25)	4213(22)	4282(23)
C(49)	8945(25)	4346(22)	4715(23)
C(50)	8969(25)	4717(22)	5310(23)
C(51)	8081(25)	4955(22)	5471(23)
C(52)	7168(25)	4822(22)	5037(23)
C(53)	7144(25)	4451(22)	4443(23)
C(54)	9290(32)	3673(15)	3317(21)
C(55)	9796(32)	3088(15)	3359(21)
C(56)	10753(32)	3055(15)	3200(21)
C(57)	11205(32)	3606(15)	2999(21)
C(58)	10700(32)	4191(15)	2958(21)
C(59)	9742(32)	4225(15)	3117(21)

1934(sh) cm^{-1}. $^{31}P\{^1H\}$ NMR: $\delta(CH_2Cl_2)$ −12.5 (s, Ir–PEt_3). FAB MS: 748, $[M]^+$, 28; 720, $[M-CO]$, 62; 692, $[M-2CO]^+$, 16; 664, $[M-3CO]^+$, 100; 636, $[M-4CO]^+$, 78; 608, $[M-5CO]^+$, 13; 580, $[M-6CO]^+$, 24; 552, $[M-7CO]^+$, 31; 524, $[M-8CO]$, 9.

Crystallography

Intensity data for **8**, **9** and **12** were measured at room temperature on an Enraf-Nonius CAD4F diffractometer fitted with graphite-monochromated Mo-K_α radiation, $\lambda = 0.7107$ Å, employing the $\omega:2\theta$ scan technique. Monitoring of three standard reflections during each data collection indicated that for **9** and **12**, decreases of 25 and 10%, respectively, in the net intensities of these standards had occurred; these data sets were scaled assuming a linear decrease in intensities. Corrections were applied for Lorentz and polarisation effects and for absorption with the use of an analytical procedure [27]. Crystal data for each compound are summarised in Table 3.

The structure of **8** was solved by interpretation of the Patterson synthesis while structure solutions for **9** and **12** were achieved by employing direct methods [27]. Each structure was refined by a full-matrix least-squares procedure based on F [27]. Phenyl rings were refined as hexagonal rigid groups with individual isotropic thermal parameters. For the refinements of **8** and **12** the remaining non-hydrogen atoms were refined with anisotropic thermal parameters except for C(9) in **12**. Attempts to refine C(9) anisotropically resulted in non-positive definite values and hence this atom was fixed in a position located from a difference map and refined isotropically. In **9** only the Fe, Ir and P atoms were refined anisotropically with the remaining atoms refined with isotropic thermal parameters. The positions of many cluster-bound carbon atoms in **9** were poorly defined and hence were refined with constrained bond distances such that Ir–C(1,2,3,4), Fe–C(5,6,7) and C(8)–C(9) were

Table 6

Fractional atomic coordinates ($\times 10^5$ for Ir; $\times 10^4$ for remaining atoms) for $Fe_2Ir(\mu_3$-$PhC_2PEt_3)(CO)_7(PEt_3)$ (**12**)

Atom	*x*	*y*	*z*
Ir	20972(6)	16795(5)	19124(5)
Fe(1)	3041(2)	4006(2)	1577(2)
Fe(2)	3159(2)	3542(2)	3240(2)
P(1)	1385(4)	−197(4)	2554(3)
P(2)	6137(4)	3961(4)	2224(3)
C(1)	2402(17)	897(18)	765(15)
O(1)	2718(14)	469(13)	12(10)
C(2)	287(17)	1837(15)	1645(12)
O(2)	−734(12)	1930(14)	1484(10)
C(3)	1451(18)	4343(17)	1273(14)
O(3)	463(14)	4566(15)	1055(12)
C(4)	3425(17)	3543(16)	429(12)
O(4)	3649(15)	3304(14)	−333(10)
C(5)	3593(17)	5662(16)	1694(14)
O(5)	3770(14)	6774(12)	1769(12)
C(6)	2987(15)	2870(17)	4259(15)
O(6)	2776(14)	2416(14)	4911(11)
C(7)	1640(16)	4026(16)	3168(13)
O(7)	635(12)	4396(13)	3224(10)
C(8)	3978(15)	5042(19)	3847(14)
O(8)	4437(13)	5990(12)	4247(9)
C(9)	4379(14)	3383(13)	2167(11)
C(10)	3981(14)	2114(13)	2446(11)
C(11)	4805(10)	1147(9)	2758(5)
C(12)	5105(10)	187(9)	2082(5)
C(13)	5818(10)	−737(9)	2338(5)
C(14)	6230(10)	−701(9)	3270(5)
C(15)	5929(10)	260(9)	3946(5)
C(16)	5216(10)	1184(9)	3690(5)
C(17)	2395(18)	−798(16)	3404(14)
C(18)	1852(20)	−1983(18)	3771(18)
C(19)	−155(17)	−170(20)	3064(15)
C(20)	−202(21)	839(25)	3853(17)
C(21)	1049(22)	−1653(15)	1675(13)
C(22)	36(23)	−1612(20)	877(15)
C(23)	6584(19)	3619(21)	1021(15)
C(24)	6295(23)	2299(22)	561(17)
C(25)	6474(18)	5662(16)	2466(17)
C(26)	7879(16)	6254(18)	2413(19)
C(27)	7330(17)	3371(18)	2907(15)
C(28)	7413(22)	3877(19)	3953(13)

1.90(2), 1.77(2) and 1.40(2) Å, respectively. Hydrogen atoms were included in the models of **8** and **12** at their calculated positions and a weighting scheme of the form $w = k/[\sigma^2(F) + g(F)^2]$ was introduced for each refinement. Final refinement details are listed in Table 3.

Neutral atomic scattering factors for Fe and Ir (corrected for f' and f'') were from ref. 28 and those for the remaining atoms were as incorporated in the SHELX 76 programme. Fractional atomic coordinates are listed in Tables 4–6 and the numbering schemes employed are shown in Figures 1–3, which were drawn with PLUTO [29]. Listings of thermal parameters, hydrogen atom parameters, all bond distances and angles and tables of observed and calculated structure factors are available from the authors (ERTT).

Acknowledgements

We are grateful for support from the Australian Research Council and for a Commonwealth Post-Graduate Research Award (to G.A.K.).

References

1 S.T. Chacon, W.R. Cullen, M.I. Bruce, O. bin Shawkataly, F.W.B. Einstein, R.H. Jones and A.C. Willis, Can. J. Chem., 68 (1990) 2001.
2 P.A. Roberts, G.R. Steinmetz, M.J. Breen, P.M. Schulman, E.D. Morrison, M.R. Duttera, C.W. de Brosse, R.R. Whittle and G.L. Geoffroy, Organometallics, 2 (1983) 846.
3 A.M. Crespi, M. Sabat and D.F. Shriver, Inorg. Chem., 27 (1988) 812.
4 E. Guggolz, M.L. Ziegler, W. Kalcher, J. Plank, D. Riedel and W.A. Herrmann, Z. Naturforsch. B, 36 (1981) 1053.
5 R. Della Pergola, L. Garlaschelli, F. Demartin, M. Manassero, N. Masciocchi, M. Sansoni and A. Fumagalli, J. Chem. Soc., Dalton Trans., (1989) 1109.
6 R. Della Pergola, L. Garlaschelli, F. Demartin, M. Manassero, N. Masciocchi and M. Sansoni, J. Chem. Soc., Dalton Trans., (1990) 127.
7 E. Sappa, A. Tiripicchio and P. Braunstein, Coord. Chem. Rev., 65 (1985) 219.
8 A. Strawczynski, R. Ros, R. Roulet, F. Grepioni and D. Braga, Helv. Chim. Acta, 71 (1988) 1985.
9 A.J. Carty, A.A. Cherkas and L.H. Randall, Polyhedron, 7 (1988) 1045.
10 E. Rosenberg, J. Bracker-Novak, R.W. Gellert, S. Aime, R. Gobetto and D. Osella, J. Organomet. Chem., 365 (1989) 163.
11 S. Aime, R. Bertoncello, V. Busetti, R. Gobetto, G. Granozzi and D. Osella, Inorg. Chem., 25 (1986) 4004.
12 D.F. Shriver and K.H. Whitmire in G. Wilkinson, F.G.A. Stone and E.W. Abel (Eds.), Comprehensive Organometallic Chemistry, Pergamon Press, Oxford, 1982, ch. 31.1.
13 N.A. Ustynyuk, V.N. Vinogradova, V.N. Korneva, D.N. Kravtsov, V.G. Andrianov and Yu.T. Struchkov, J. Organomet. Chem., 277 (1984) 285.
14 K. Yasufuku and H. Yamazaki, Bull. Chem. Soc. Jpn., 45 (1972) 2664.
15 (a) R. Mason, I. Søtofte, S.D. Robinson and M.F. Uttley, J. Organomet. Chem., 46 (1972) C61; (b) P.L. Bellon, C. Benedicenti, G. Caglio and M. Manassero, J. Chem. Soc., Chem. Commun., (1973) 946.
16 J.F. Tilney-Bassett, J. Chem. Soc., (1963) 4784.
17 M.J. Mays, P.R. Raithby, P.L. Taylor and K. Henrick, J. Chem. Soc., Dalton Trans., (1984) 959.
18 K. Henrick, M. McPartlin, A.J. Deeming, S. Hasso and P. Manning, J. Chem. Soc., Dalton Trans., (1982) 899.
19 Y.S. Wong, H.N. Paik, P.C. Chieh and A.J. Carty, J. Chem. Soc., Chem. Commun., (1975) 309.
20 P.S. Pregosin in J.G. Verkade and J.G. Quin (Eds.), Phosphorus-31 NMR Spectroscopy in Stereochemical Analysis: Organic Compounds and Metal Complexes, VCH, New York, 1986, ch. 14.
21 J.C. Tebby in J.G. Verkade and J.G. Quin (Eds.), Phosphorus-31 NMR Spectroscopy in Stereochemical Analysis: Organic Compounds and Metal Complexes, VCH, New York, 1986, ch. 1.
22 T. Albiez and H. Vahrenkamp, Angew. Chem., Int. Ed. Engl., 26 (1987) 572.
23 M.I. Bruce, M.L. Williams, B.W. Skelton and A.H. White, J. Organomet. Chem., 369 (1989) 393.
24 R.H. Walter and B.F.G. Johnson, J. Chem. Soc., Dalton Trans., (1978) 381.
25 M.I. Bruce, M.G. Humphrey, J.G. Matisons, S.K. Roy and A.G. Swincer, Aust. J. Chem., 37 (1984) 1955.
26 A.F. Clifford and A.K. Mukherjee, Inorg. Synth., 8 (1966) 186.

27 G.M. Sheldrick, SHELX76—Programme for Crystal Structure Determination, University of Cambridge, 1976.

28 J.A. Ibers and W.C. Hamilton, International Tables for X-Ray Crystallography, Vol. 4, Kynoch Press, Birmingham, 1974.

29 W.D.S. Motherwell, PLUTO–Plotting Programme for Molecular Structures, University of Cambridge, 1978.